IEEE Access
Multidisciplinary | Rapid Review | Open Access Journal

Received June 21, 2021, accepted August 6, 2021, date of publication August 9, 2021, date of current version August 16, 2021.

Digital Object Identifier 10.1109/ACCESS.2021.3103859

Design of Enhanced Permutation Differential Chaos Shift System Using Signal Reference With Dual Modulation

NIZAR AL BASSAM[1] **AND ODAY AL-JEREW**[2]
[1]Middle East College, Muscat 124, Oman
[2]Asia Pacific International College, Sydney, NSW 2150, Australia
Corresponding author: Nizar Al Bassam (rsarsa76@gmail.com)

ABSTRACT In this paper, a permutation-based chaos system, named as Single Reference Permutation Index with Dual Modulation Differential Chaos Shift Keying (SR-PIDM-DCSK), is developed and tested. The proposed system uses the chaotic segment and its reversed version to modulate two pairs of data sets simultaneously. It uses the same reference for multiple symbol modulation. This significantly reduces bit energy requirement and enhances the Bit Error Rate (BER). In addition, it reduces the complexity of the system. At the transmitter, the reference signal is sent first, then the same reference is delayed and permutated to send the first information set of bits, while the same version is time reversed and permutated to modulate the second set of bits. Both segments are added together on the same symbol duration slot for transmission. This process is repeated for multiple symbols in a frame. At the receiver, the incoming reference signal is delayed for several symbol durations for demodulation. The BER of the system is evaluated in various channel environments. Moreover, a theoretical prediction for BER formula is developed for the suggested model. Results show that the proposed system has superior BER performance compared with other standard chaos based systems by an average of 2 dB. It is evident that the BER performance is enhanced with the increase in the spreading factor and the number of symbols in a frame. The theoretical formula for BER prediction is validated by computer simulation. Excellent matching was found between the theoretical formula and simulation results.

INDEX TERMS AWGN channel, differential coherence, differential correlator, permutation index.

I. INTRODUCTION

The chaos communications system is based on using a chaotic signal, which has the main function of carrying information signals to help recover the information signal through modulation and demodulation processes. The chaos signal is random-like, with a non-repeated pattern and bounded values. Hence, chaos-based communication systems can be classified as coherent, non-coherent, and differentially coherent systems [1], [2].

Recently, differentially coherent systems have attracted researchers' attention as they have attempted to explore the potential of using them in practice due to their features. These features include high BER performance, resistance to multipath fading, and anti-jamming capability required to send a reference chaotic signal for each information-bearing signal. This reduces bandwidth efficiency concerning data rate by almost 50%. In coherent systems, the receiver does not require a reference part since the carrier signal is locally generated at the receiver. However, synchronization is a very challenging task, particularly in the presence of high noise levels. In non-coherent systems, accurate estimation of the carrier statical parameters of a transmitted signal such as power is necessary to differentiate between the transmitted signals. However, threshold optimization is another challenge. Based on the previous discussion, a different coherent system is preferred [2].

To overcome the challenge of synchronization in differentially coherent systems, Differential Coherent Shift Keying (DCSK) and Correlation Delay Shift Keying (CDSK) are suggested as the basic building blocks [1], [3], [4]. Several systems have been developed to overcome the drawbacks of low bit rate and low spectral efficiency as follows:

- *Adding reference and information bearing signals to the same time slots*: the schemes are designed to combine and add both; reference and information signals on

The associate editor coordinating the review of this manuscript and approving it for publication was Sun Junwei.

the same time slots utilize the orthogonality between the chaotic signal and its time-shifted version as in HE-DCSK [5] and reference modulated DCSK [6]. The major disadvantage of these systems is having intra-signal interference which degrades the performance.

- *Information bit coding*: coding has been used to separate reference and information bearing signals by keeping the orthogonality. One way is to implement the Walsh code as in [7], [8] or Space-Time Block Code – DCSK (STBC-DCSK) to improve the BER performance and data rate as in [9]. Photograph low density party check code is used to improve the channel capacity as in coded DCSK [10].
- *Using of multicarrier modulation*: the OFDM multicarrier systems have been discussed initially in [11] while an enhanced version to avoid the PAPR occurring in MC-DCSK systems has been proposed in [12]. One non-information bearing reference sub-carrier signal is proposed to achieve high energy saving in the system spectrum. The work in [13] is designed to implement the OFDM-based orthogonal chaotic vector shift keying scheme. The scheme utilizes multiple orthogonal chaos signal generators to model multiple information bits. The use of a multicarrier system offers a high data rate, but it requires more complex receivers in terms of filter design and carrier synchronization requirements. The system in [14] improved the BER by proposing iterative demodulation, while Repeated Spreading Sequence (RSS) is the basic block of the proposed multicarrier system. A theoretical information capacity limit is derived and simulated in [15].

Since any chaotic signal and its time permutated version have very low correlation, this offers an opportunity to build M-ARY modulation scheme for DCSK and enhance the security as in [16], [17]. The system is based on sending one single reference signal followed by a permutated version of the information-bearing signal. The permutation arrangement depends on the transmitted data set. At the receiver, the incoming signal undergoes all permutation possibilities and correlates with the delayed version of the received signal as described in PI-DCSK [18]. The multi-carrier M-ary differential chaos shift keying (M-DCSK) system is proposed in [19]. The reference and information-bearing signals for each subcarrier are transmitted simultaneously. The reference signals are coded by a Walsh code to carry additional information bits, hence improving data rate. The system is derived over additive white Gaussian noise and multipath Rayleigh fading channels. A M-ary DCSK system with replica piecewise frame to resist impulsive noise is proposed in [20]. Using Gaussian Q-function to model the BER of the M-DCSK system is proposed in [21]. The authors applied the Remez algorithm to achieve the minimax approximation for the derived BER form over multipath Rayleigh fading channels. Improved versions of PI-DCSK where reference chaotic segment and information-bearing signals are combined on one-bit duration are presented in [22]. Walsh code is also recalled in [23] to separate reference and information bearing signals. Using a superposition coding principle on the reference and the information-bearing signals to achieve multi-user simultaneous information transmission is proposed in [24]. The proposed system is suitable for downlinking multi-user short-range wireless communications. The wireless information and power transfer (SWIPT) system is suggested in [25]. The system is based on simultaneously carrying information and energy to provide energy supply for power-limited devices. The proposed system achieves anti-multipath fading capability without using channel estimators.

In this brief, a common reference signal is used to modulate the frame of information symbols, each symbol consisting of two parts. The first part is a normal permutation M-ARY DCSK system while the second part modulates other sets using a time reverse version of the same reference signal. Both parts are added together at the same time slot. The modulation process is repeated for several symbols in the same data frame. Thus, the proposed system enhances the energy efficiency and offers higher bit rates compared with the standard PI-DCSK systems. The contributions of this paper are summarized as follows:

1) We propose a framework of SR-PIDM-DCSK system, which uses a common reference signal to modulate multiple data symbols. This is unlike the PI-DCSK where each information-bearing signal is sent with a dedicated reference signal. The proposed scheme is an active combination of the PI-DCSK and I-DCSK [16], [26] which uses a common reference signal. This arrangement significantly saves energy requirements compared with the standard differential coherent system.
2) A theoretical model is derived to predict the bit error performance in the common AWGN channel. The analytical results and simulation illustrate that the proposed system outperforms the other systems significantly at large frame size.

The rest of this paper is organized as follows: Section II gives the proposed SR-PIDM-DCSK system. Section III and Section IV analyze the performance of the proposed system. The proposed system complexity analysis is evaluated in Section V. System simulation and discussion are provided at Section VI. Finally, Section VII concludes the paper.

II. THE PROPOSED SCHEME SR-PIDM-DCSK

The modulator and demodulator design for the SR-PIDM-DCSK system are shown in Fig. 1 and Fig. 2, respectively. The chaotic source generates a signal with a length of M samples at each i^{th} instant, where M is the spreading factor. The transmitted reference signal can be given as $X_o = \{x_1\ x_2\ \ldots x_M\}$.

To transmit the first information symbol, the generated reference signal is delayed by one symbol duration and passed to the information mapping process in the first arm (as shown in Fig. 1) through two operations, mapping

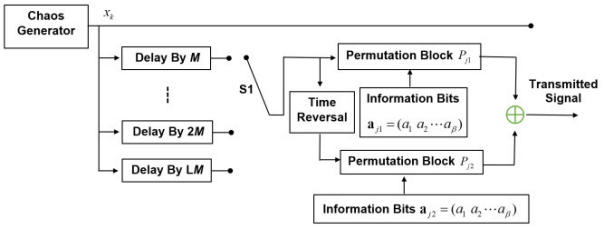

FIGURE 1. SR-PIDM-DCSK transmitter block diagram.

and time reversal. The delayed version of the reference signal is mapped to the first information set while the time reversed version is also subjected to the mapping operation in the second arm as shown in Fig. 1. Both mapped signals are added together in the same time slot which is equal to one symbol duration. Later, the reference signal is delayed by the second time duration to proceed with the next information symbol in the same frame.

Orthogonality between the reference signal and its permutated version is maintained such that $XP_j{}^T(X) = 0$ and $X'P_j{}^T(X') = 0$. This also applicable for $P(X^T) \neq X'$ [17]. Permutation is performed through $P(.)$ where P is $M \times M$ permutation matrix. X' is the time reversal version of the chaotic segment X given by $X_o{}' = \{x'_1 x'_2 \ldots x'_M\}$ such that $x'_1 = x_M, x'_2 = x_{M-1}$ while $x'_M = x_1$.

For a chaotic segment having length of M samples, there is a possibility of $M! - 1$ permutations. Therefore, information mapping is performed by selecting one unique chaotic permutation for each data set such that $\mathbf{a_{j1}} \rightarrow P_{\mathbf{j1}}$ and $\mathbf{a_{j2}} \rightarrow P_{\mathbf{j2}}$. P_{j1} and P_{j2} are the selected permutation matrices applied on the chaotic sequence and its time reversal version respectively. Where $\mathbf{a_{j1}}$ and $\mathbf{a_{j2}}$ are the transmitted data set selected from $\mathbf{a}_j = (a_1\ a_2 \ldots a_\beta)$, where β is the number of bits per symbol. Therefore, the first transmitted frame, S, can be given by the baseband representation as:

$$S = [\ \underbrace{X_0}_{reference}\ \underbrace{P_{j1}(X_M{}^T) + P_{j2}(X'_M{}^T)}_{\text{First Information Bearing Signal}}\ \underbrace{P_{j3}(X_{2M}{}^T) + P_{j4}(X'_{2M}{}^T)}_{\text{Second Information Bearing Signal}}\ \cdots\ \underbrace{P_{j2L-1}(X_{(L-1)M}{}^T) + P_{j2L}(X'_{LM}{}^T)}_{\text{L}^{\text{th}}\text{ Information Bearing Signal}}\ ] \quad (1)$$

Assume X_q is the chaotic vector delayed by q samples such that $X_q = \left(x_{1-q}, x_{2-q} \ldots x_{M-q}\right)$. The rest of the paper will consider the analysis of the first pair of information symbols in the first frame since all the information sets are statistically independent. Hence the first received symbol can be written as $R = S + N$, where N is the noise vector added to the transmitted signal which can be given as $N = n_o\ n_1 \cdots n_{(L+1)M}$, where n_i is the i^{th} noise sample with the PSD $N_o/2$.

The receiver design is shown in Fig. 2, consisting of a bank of permutation-based correlators. The correlators in the first part are used to decode the information symbols in the

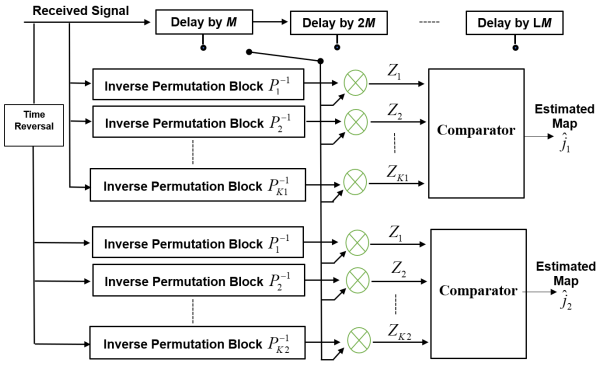

FIGURE 2. SR-PIDM-DCSK receiver diagram.

forward chaotic signal while, in the second part, correlation is performed after the time reversal. The process can be illustrated as follows:

1) The incoming reference signal is loaded into the delay block and stored for correlation for the L^{th} successive symbol duration.
2) First, the information-bearing signal is received and permutated for all $K1 = K2 = 2^\beta$ possibilities.
3) The output of the $k1^{th}$ permutation block is multiplied with the reference signal, then the comparator selects the highest output that represents the possible transmitted set in the forward segment.
4) A copy of the same information-bearing signal undergoes time reversal before permutations.
5) Steps 2 and 3 are repeated to decode the information in the time reverse version of the information-bearing signal.
6) The reference signal is kept for additional symbol duration to decode the information in the next symbols.

The output of first correlator is given by $P_{k1}{}^{-1}(P_{j1}X_M + N_0)$. Therefore, the $k1^{th}$ correlator outputs can be given as

$$Z_{k1} = (X_M + N_M)P_{k1}{}^{-1}(P_{j1}X_M{}^T + P_{j2}X'^T_M + N_0) \quad (2)$$

While the output of the second arm can be given by

$$Z_{k2} = (X_M + N_M)P_{k2}{}^{-1}(P_{j1}X'^T_M + P_{j2}X_M{}^T + N_0') \quad (3)$$

The correlator output can be expanded to

$$Z_{k1} = (\underbrace{X_M P_{k1}^{-1} P_{j1} X_M{}^T}_{SS1} + \underbrace{X_M P_{k1}^{-1} P_{j2} X'_M{}^T}_{SI1} + \underbrace{X_M P_{k1}^{-1} N_M + N_M P_{k1}^{-1} P_{j1} X_M{}^T + N_M P_{k1}^{-1} P_{j2} X'_M{}^T}_{SN1} + \underbrace{N_M P_{k1}^{-1} N_M}_{NN1}) \quad (4)$$

$$Z_{k2} = (\underbrace{X_M P_{k2}{}^{-1} P_{j1} X'_M{}^T}_{SS2} + \underbrace{X_M P_{k2}{}^{-1} P_{j2} X_M{}^T}_{SI2} + \underbrace{X_M P_{k2}^{-1} N'_M + N_M P_{k2}^{-1} P_{j1} X'_M{}^T + N_M P_{k2}^{-1} P_{j2} X_M{}^T}_{SN2} + \underbrace{N_M P_{k2}^{-1} N'_M}_{NN2}) \quad (5)$$

The $SS1$ and $SS2$ represent the useful signal components given at $k_1 = j_1$ and $k_2 = j_2$, respectively. Correlation between chaotic signal and time permutated version resulted in correlator inter-signal interference terms given by SI_1 and SI_2. The cross correlation between noise and the chaotic signal is given by the terms $SN1$ and $SN2$. $NN1$ and $NN2$ represent the noise power contribution at the correlator output which has a significant impact on performance, particularly at a large spreading factor of M.

The estimated permutation index $\hat{j}_1$ and $\hat{j}_2$ in the decision circuit can be calculated

$$\hat{j}_1 = \arg\ \max\ \{Z_{k1}\},\ k1 \in \{1, 2, \cdots 2^{\beta}\} \tag{6}$$

Similarly,

$$\hat{j}_2 = \arg\ \max\ \{Z_{k2}\},\ k2 \in \{1, 2, \cdots 2^{\beta}\} \tag{7}$$

III. SYSTEM ANALYSIS

Energy efficiency improvement of the proposed scheme can be analysed by calculating the Data energy to Bit energy measure Ratio (DBR) which is defined in [18]. The measure is used to evaluate the efficiency in energy saving with respect to number of transmitted information bits and is given by

$$DBR = E_{data}/E_b \tag{8}$$

where E_{data} is the energy of the data bearing signal, while E_b represents the total bit energy required to carry each information bit. In other words, it is the ratio between the number of transmitted chaotic sequence to the number of transmitted bits. Assuming equal spreading factor (i.e chip rate T_c) in all systems. In the proposed scheme, a reference signal is used to transmit $2L$ symbols in each frame. L symbols are transmitted using a copied version of the reference signal, while the other L symbols are sent using the time reversal version. Where each symbol carrier β data. Hence, the average energy per symbol E_s is given by

$$E_s = E_{data} + \frac{E_{ref}}{2L} \tag{9}$$

The Average energy for information bearing data signal can be calculated as

$$E_{data} = M \sum_{i=1}^{M} x_i^2 = MV(x) \tag{10}$$

where $V(x)$ is the variance of the chaotic signal. Since reference signal is used for $2L$ symbols, therefore

$$E_{ref} = \frac{M}{2L} \sum_{i=1}^{M} x_i^2 = \frac{M}{2L} V(x) \tag{11}$$

Then the total average energy per symbol can be given by

$$E_s = M(1 + \frac{1}{2L})V(x) \tag{12}$$

Since each symbol is used to transmit β bits

$$\beta E_b = M(1 + \frac{1}{2L})V(x) \tag{13}$$

$$E_b = \frac{M}{2L\beta}(2L + 1)V(x) \tag{14}$$

TABLE 1. DBR comparison of different chaotic modulation techniques.

Modulation Scheme	DBR
DCSK	1/2
CDSK	1/2
HE-DCSK	2/3
I-DCSK	1/2
PI-DCSK	$\beta/2$
HE-PIDCSK	$2\beta/3$
HE-DMPI-DCSK	β

Substituting 9 and 14 into equation 8, then

$$\frac{E_{data}}{E_b} = \frac{MV(x)}{\frac{M}{2L\beta}(2L + 1)V(x)} = \frac{2L\beta}{(2L + 1)} \simeq \beta \tag{15}$$

With respect to differentially coherence systems, each symbol is presented by two chaotic segment such as DCSK, CDSK, I-DCSK and HE-DCSK, while in permutation based systems, energy efficiency is increased since the same chaotic segment is used to transmit β bits. Table 1 illustrates the DBR for various chaotic modulation scheme used in this paper. To have a fair comparison between systems, the BER performance is evaluated under fixed E_b/N_o and with the same spreading factor M (i. e chip rate).

Assuming the noise is AWGN having PSD equal $N_o/2$, then E_b/N_o can be

$$E_b/N_o = \frac{M(2L + 1)V(x)}{4L\beta V(n)} \tag{16}$$

IV. PERFORMANCE ANALYSIS

In this section, the theoretical prediction formula for BER is derived for the SR-PIDM-DCSK system using the GA method, which fits a system having a large spreading factor. The derivation assumes the transmitter and receiver are perfectly synchronized in the AWGN channel environment.

Symmetric tent map is described by the equation $x_{i+1} = 1 - 2|x_i|$ which is selected to derive the chaotic source. The sequence is stationary and is uniformly distributed from $(-1, 1)$ with zero mean and computed variance $V(x) = 1/3$ and $V(x^2) = 4/45 = 4/5\ V^2(x)$ [6].

The following assumptions are considered to derive BER theoretical performance in its final form:

1) That chaotic sample x_i and its time mirrored version x_i' are statistically independent from the noise sample n_i for all i.
2) The correlation between the chaotic sample X and its permutated version $P_j X^T$ or time reversed permutated $P_j X'^T$ tends to decay quickly as spreading factor M increases.

In each SR-PIDM-DCSK symbol, β bits are mapped into a distinguished permutation of the chaotic sample while another β bits are mapped to the time reversal-permutated version. Both symbols are added together in the same time slots. The operation is repeated for L symbols in each frame. Since information symbols are statistically independent, the BER of SR-PIDM-DCSK is based on average error probability. The error probability in correct segment detection

$P_{r_{ed}}$ at any $k1^{th}$ correlator output and error in permutation estimation Pr_{map} is given by

$$P_{map} = \frac{2^{(\beta-1)}}{2^{\beta}-1} P_{r_{ed}} \tag{17}$$

Permutation index of the first transmitted symbol is performed by selecting the maximum absolute values from the output of correlators. The output of each correlator equals the correlation between the received signal, which undergoes all possible permutations, and the delayed version of the reference signal. For the second permutation index of the same symbol, the process is repeated, but after the time reversing process as shown in Fig. 2

Each correlator output can be modeled as a Gaussian random variable Z_{k1} and Z_{k2}. For equiprobable transmitted sequence, the error probability of permutation index estimation conditioned by P_{j1} and P_{j2} can be given by

$$P_{red} = (P_r|Z_{j1}| < \max P_r|Z_{k1}|) \text{ for } 1 \le k1 \le 2^{\beta}, \tag{18}$$

or

$$P_{red} = (P_r|Z_{j2}| < \max P_r|Z_{k2}|) \text{ for } 1 \le k2 \le 2^{\beta}. \tag{19}$$

where the Z_{j1} and Z_{k1} are decision variable at the $j1^{th}$ and $k1^{th}$ correlator output, where $j1 \neq k1$.

The error will occur only if any value of Z_{k1} can have a magnitude larger the Z_{j1} in the first correlator, the output of $k1^{th}$ correlator can be rewritten as

$$Z_{k1} = SS1 + SI1 + SN1 + NN1 \tag{20}$$

The correlation components can be calculated as

$$\begin{aligned} Z_{k1} = & (\underbrace{X_M P_{k1}^{-1} P_{j1} X_M^T}_{SS1} \\ & + \underbrace{X_M P_{k1}^{-1} P_{j2} X'^T_M}_{SI1} \\ & + \underbrace{X_M P_{k1}^{-1} N_M + N_M P_{k1}^{-1} P_{j1} X_M^T + N_M P_{k1}^{-1} P_{j2} X'^T_M}_{SN1} \\ & + \underbrace{N_M P_{k1}^{-1} N_M}_{\mathrm{NN1}}) \end{aligned} \tag{21}$$

$$\begin{aligned} SS1 &= X_M {P_{k1}}^{-1} P_{j1} {X_M}^T \\ &= \sum_{b=1}^{M}\sum_{a=1}^{M}\sum_{i=M+1}^{2M} p_{k1}^{b,a} p_{j1}^{a,b} {x^2}_{i-M}, \end{aligned} \tag{22}$$

where a and b are the indexes of the permutation matrix.

$$\begin{aligned} SI_1 &= X_M {P_{k1}}^{-1} P_{j2} X'^T_M \\ &= \sum_{a=1}^{M}\sum_{b=1}^{M}\sum_{i=M+1}^{2M} x_{i-M} p_{k1}^{b,a} p_{j1}^{a,b} {x'}_{i-M} \end{aligned} \tag{23}$$

$$\begin{aligned} & X_M {P_{k1}}^{-1} N_M + N_M {P_{k1}}^{-1} P_{j1} {X_M}^T + N_M {P_{k1}}^{-1} P_{j2} X'^T_M \\ &= \sum_{b=1}^{M}\sum_{a=1}^{M}\sum_{i=M+1}^{2M} x_{i-M} p_{k1}^{b,a}\, n_{i-M} \\ &\quad + \sum_{b=1}^{M}\sum_{a=1}^{M}\sum_{i=M+1}^{2M} n_{i-M} p_{k1}^{b,a} p_{j1}^{a,b}\, x_{i-M} \\ &\quad + \sum_{b=1}^{M}\sum_{a=1}^{M}\sum_{i=M+1}^{2M} n_{i-M} p_{k1}^{b,a} p_{j2}^{a,b}\, {x'}_{i-M} \end{aligned} \tag{24}$$

$$\mathrm{NN1} = N_M {P_{j1}}^{-1} N_0 = \sum_{b=1}^{M}\sum_{a=1}^{M}\sum_{i=M+1}^{2M} n_{i-M} p_{j1}^{b,a}\, n'_{i-M}, \tag{25}$$

where n' is the permutated noise sample.

Based on assumptions 1 and 2 (in Section IV), the mean and variance of the correlator output conditioned by $k_1 = j_1$ can be given by

$$\begin{aligned} E(Z_{j1}) &= E(SS1) + E(SI1) + E(SN1) + E(NN1) \\ &= \sum_{i=M+1}^{2M} {x^2}_{i-M} + 0 + 0 + 0 \\ &= MV(x) = E_s \end{aligned} \tag{26}$$

$$E_s = \frac{2L\beta}{(2L+1)} E_b \tag{27}$$

$$V(Z_{j1}) = V(SS1) + V(\mathrm{SI1}) + V(SN1) + V(\mathrm{NN1}) \tag{28}$$

$$\begin{aligned} V(SS1) &= V(\sum_{b=1}^{M}\sum_{a=1}^{M}\sum_{i=M+1}^{2M} p_{k1}^{b,a}\, p_{j1}^{a,b}\, {x^2}_{i-M}) \\ &= \frac{4}{45} M = \frac{4}{5} MV(x).V(x) \\ &= \frac{4E_s^2}{5M} \\ &= \frac{4}{5M}\left(\frac{4L^2\beta^2}{(2L+1)^2} E_b^2\right) = \frac{16L^2\beta^2}{5M(2L+1)^2} E_b^2 \end{aligned} \tag{29}$$

$$\begin{aligned} V(\mathrm{SI1}) &= \sum_{b=1}^{M}\sum_{a=1}^{M}\sum_{i=M+1}^{2M} x_{i-M} p_{k1}^{b,a} p_{j1}^{a,b} {x'}_{i-M} \\ &= MV(x)V(x) = \frac{E_s^2}{M} = \frac{4L^2\beta^2}{M^2(2L+1)^2} E_b^2 \end{aligned} \tag{30}$$

$$\begin{aligned} V(SN1) &= V(\sum_{b=1}^{M}\sum_{a=1}^{M}\sum_{i=M+1}^{2M} x_{i-M} p_{k1}^{b,a}\, n_{i-M} \\ &\quad + \sum_{b=1}^{M}\sum_{a=1}^{M}\sum_{i=M+1}^{2M} n_{i-M} p_{k1}^{b,a} p_{j1}^{a,b}\, x_{i-M} \\ &\quad + \sum_{b=1}^{M}\sum_{a=1}^{M}\sum_{i=M+1}^{2M} n_{i-M} p_{k1}^{b,a} p_{j1}^{a,b}\, {x'}_{i-M}) \\ &= 3MV(x)V(n) \\ &= \left(\frac{6L\beta}{(2L+1)} E_b\right)\frac{N_o}{2} = \frac{3L\beta}{(2L+1)} E_b N_o \end{aligned} \tag{31}$$

$$V(\mathrm{NN}) = V(n).V(n') = \frac{M}{4} N_o^2 \tag{32}$$

$$\begin{aligned} V(Z_{j1}) = & \frac{16L^2\beta^2}{5M(2L+1)^2} E_b^2 + \frac{4L^2\beta^2}{M^2(2L+1)^2} E_b^2 \\ & + \frac{3L\beta}{(2L+1)} E_b N_o + \frac{M}{4} N_o^2 \end{aligned} \tag{33}$$

For any $k1^{th}$ correlator output conditioned by $k_1 \neq j_1$, the mean and variance of the correlator can be easily shown as

$E(Z_{k1}) = 0$ and

$$V(Z_{k1}) = 2MV(x)V(x) + 3MV(x)V(n) + \frac{M}{4}N_o^2 = \frac{8L^2\beta^2}{M^2(2L+1)^2}E_b^2 + \frac{3L\beta}{(2L+1)}E_bN + \frac{M}{4}N_o^2 \quad (34)$$

The output of each $2^n - 1$ correlators Z_{k1} for $k1 \neq j1$ are statistically independent random values characterized by a normal distribution with zero mean and having PDF that is given by

$$f_{Z_{k1}}(y) = \frac{1}{\sqrt{2\pi V(Z_{k1})}} e^{-\frac{(y)^2}{2V(Z_{k1})}} \quad (35)$$

While the correlator output PDF conditioned by correct permutation can be given as

$$f_{Z_{j1}}(y) = \frac{1}{\sqrt{2\pi V(Z_{j1})}} e^{-\frac{(y-E(Z_{j1}))^2}{2V(Z_{j1})}} \quad (36)$$

It is easier to calculate the probability of correct permutation which occurs only if the magnitude of $Z_{j1} > Z_{k1}$ and $Z_{j2} > Z_{k2}$ and so on; therefore, the probability of correct map detection can be given as [23]

$$p_{map} = 1 - \int_0^\infty F_{Z_{k1}}(y)^{2^\beta - 1} f_{Z_{j1}}(Z_{j1})dy \quad (37)$$

where $F_{Z_{k1}}(y)$ is the commutative distribution function given by

$$F_{Z_{k1}}(y) = erf\left(\frac{y}{\sqrt{2\pi V(Z_{k1})}}\right) \quad (38)$$

The overall BER of the system can be given by

$$BER_{SR-PIDM-DCSK} = \frac{2^{(n-1)}}{2^n - 1} \left[1 - \frac{1}{\sqrt{\frac{144}{45}E_b^2 + 2E_oN_o + \frac{\beta}{4}N_o^2}}\right. \int_0^\infty erf\left(\frac{y}{\sqrt{\frac{32}{45}E_b^2 + 2E_oN_o + \frac{\beta}{4}N_o^2}}\right)^{2^n-1} \left. e^{-\frac{(y-\frac{4}{3}E_b))^2}{2(\frac{144}{45}E_b^2 + 2E_oN_o + \frac{\beta}{4}N_o^2)}} dy\right] \quad (39)$$

V. COMPLEXITY ANALYSIS

In this section, system complexity is evaluated against a number of essential components in each system. To make a fair comparison, evaluation is calculated for hardware resources required to transmit and receive single bits. In the SR-PIDM-DCSK transmitter, as shown in Table 2, it is required to transmit $2L\beta$ bits in each frame which have a common reference; hence each symbol carries 2β bits and requires a single time reversal unit. The output of the first and second permutator is added together using only one single adder. This structure reused L times per frame; hence, SR-PIDM-DCSK system has less adder than CDSK, HE-DCSK and I-DCSK and HE-PIDCSK, however, the is no adder in DCSK and PI-DCSK. In addition, the proposed system has less complexity than DCSK, CDSK, HE-DCSK and I-DCSK in term of multipliers, delay and modulator. The DPU unit in the proposed system is also less than PI-DCSK and HE-PIDCSK while there is no DPU in DCSK, CDSK and HE-DCSK.

TABLE 2. Transmitter system complexity analysis (for one information bits).

Unit	DCSK	CDSK	HE-DCSK	I-DCSK	PI-DCSK	HE-PIDCSK	SR-PIDM-DCSK
Adders	0	1	1	1	0	$1/2\beta$	$1/2\beta L$
Multipliers	1	1	1	1	0	0	0
Delay	1	1	1	0	$1/\beta$	$1/2\beta$	$1/2\beta$
Modulator	1	1	1	1	0	0	0
DPU[a]	0	0	0	1	$1/\beta$	$1/\beta L$	$1/2\beta L$

[a]DPU: Data Permutation Unit (including the time reversal unit)

TABLE 3. Receiver system complexity analysis (for one information bit).

Unit	DCSK	CDSK	HE-DCSK	I-DCSK	PI-DCSK	HE-PIDCSK	SR-PIDM-DCSK
Multipliers	1	1	1	1	$1/2^\beta$	$1/2^{\beta+1}$	$1/2^{\beta+1}$
Delay	1	1	1	1	$1/\beta$	$1/2\beta$	$1/2\beta$
Demodulator	1	1	1	1	$1/2^\beta$	$1/2^{\beta+1}$	$1/2^{\beta+1}$
DMU [a]	0	0	0	1	2^β	$2^{\beta+1}$	$2^{\beta+1}$

[a]DMU:Data Mapping Unit (including the time reversal unit)

The receiver of the proposed scheme requires L delay element which helps to reuse the structure of receiver L times as shown in Fig. 2. Detailed receiver complexity of the SR-PIDM-DCSK compared with other systems is illustrated in Table 3. The proposed scheme is less complexity than DCSK, CDSK, HE-DCSK and I-DCSK in term of multipliers, delay and demodulator. However, other systems is less DMU complexity than SR-PIDM-DCSK. Moreover, the receiver complexity is the same in the HE-PIDCSD and the proposed system.

VI. SIMULATION RESULTS AND DISCUSSION

In this section, different chaos schemes have been simulated and compared with the proposed system over AWGN and multipath Rayleigh fading channels environments and with various E_b/N_0.

System BER performance is theoretically evaluated using the expression in Eq. (39) and validated using computer simulation. As shown in Fig. 3, theoretical evaluation is closely related to the computer simulation result at spreading factor of $M = 100$. The small variation is due to the use of the GA method which is based on averaging of bit energy and ignoring the variation. However, excellent matching can be observed clearly at higher spreading factors as shown in Fig. 4 and Fig. 5. This can be attributed to the fact the chaotic signal energy becomes an almost constant value at typical spreading.

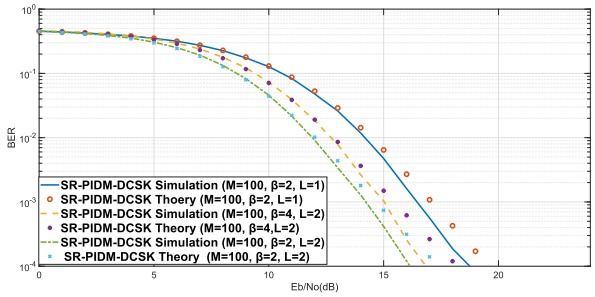

FIGURE 3. Theoretical and simulation BER results for SR-PIDM-DCSK system where $M = 100$.

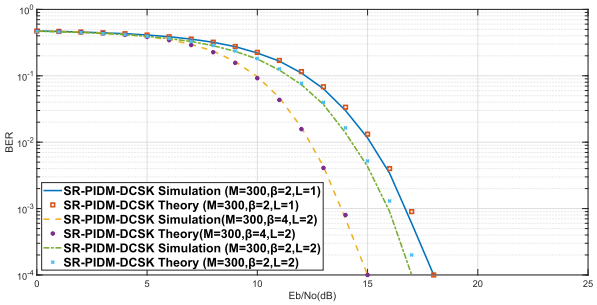

FIGURE 4. Theoretical and simulation BER results for SR-PIDM-DCSK system where $M = 300$.

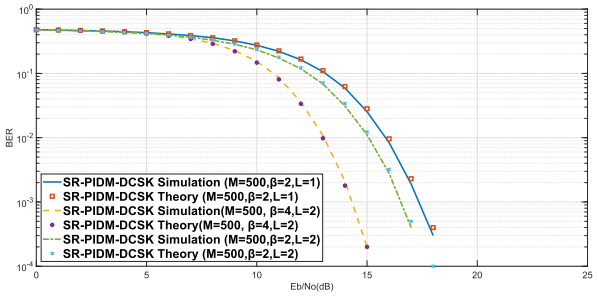

FIGURE 5. Theoretical and simulation BER results for SR-PIDM-DCSK system where $M = 500$.

The BER performance of SR-PIDM-DCSK is initially compared with other standard chaos-based systems, typically DCSK, CDSK and HE-DCSK. In addition, the SR-PIDM-DCSK is also evaluated with the permutation-based chaos systems, namely PI-DCSK, I-DCSK and HE-PIDCSK [18], [27]. All the systems are simulated using the same spreading factors and at equal E_B/N_0 levels, when transmitted over the AWGN channel environment.

At spreading factor $M = 100$, with $\beta = 2, 4$ and $L = 2, 3$, the performance of the proposed system is compared with other systems. The DCSK slightly outperforms SR-PIDM-DCSK, as shown in Fig. 6; however, the proposed system BER outperforms DCSK, CDSK, HE-DCSK, and PI-DCSK by an average of 2.5 dB at spreading factors of 150, 200, 300, and 500 as shown in Fig.s 7, 8 and 9, respectively. The reason behind such performance is the energy saving obtained from using a single reference signal for multiple information-bearing signals which features the proposed scheme, while all other systems use dedicated

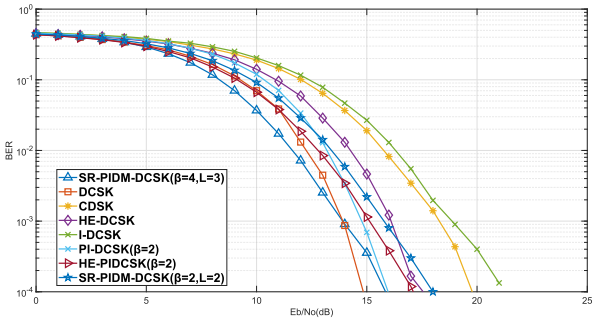

FIGURE 6. The BER results for SR-PIDM-DCSK verses DCSK, CDSK, HE-DCSK, I-DCSK, PI-DCSK and HE-PIDCSK where $M = 100$.

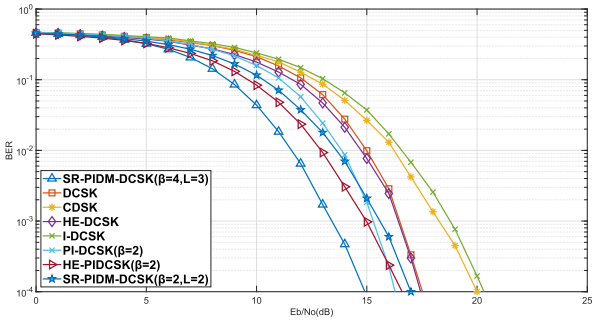

FIGURE 7. The BER results for SR-PIDM-DCSK verses DCSK, CDSK, HE-DCSK, I-DCSK, PI-DCSK and HE-PIDCSK where $M = 150$.

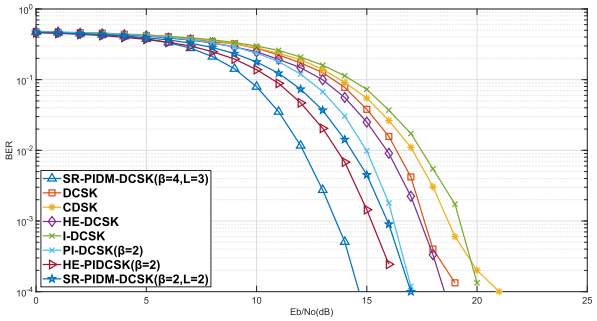

FIGURE 8. The BER results for SR-PIDM-DCSK verses DCSK, CDSK, HE-DCSK, I-DCSK, PI-DCSK and HE-PIDCSK where $M = 300$.

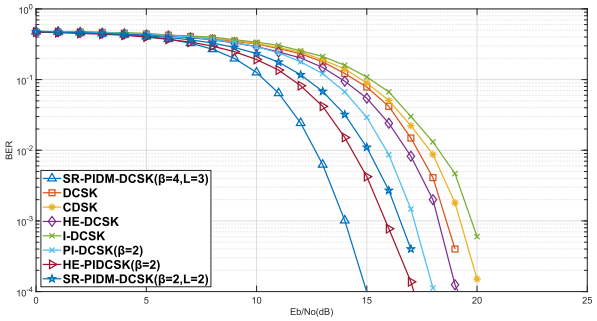

FIGURE 9. The BER results for SR-PIDM-DCSK verses DCSK, CDSK, HE-DCSK, I-DCSK, PI-DCSK and HE-PIDCSK where $M = 500$.

reference signals for each information symbol. Moreover, increasing the spreading factor enhances the orthogonality which reduces the effect of signal to signal and signal to noise interference. The overall system BER performances are decreased while spreading factors continue to increase; this is

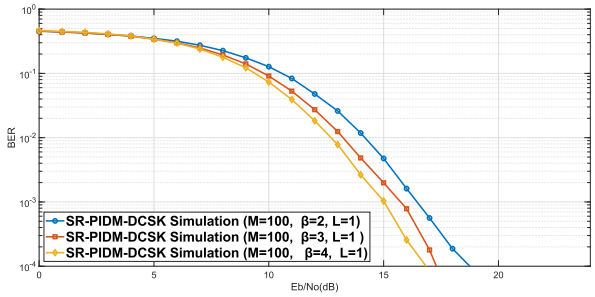

FIGURE 10. The BER results for SR-PIDM-DCSK at various bit per symbols length for one symbol per frame where $M = 100$.

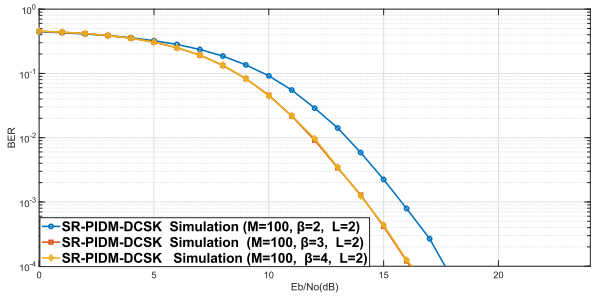

FIGURE 11. The BER results for SR-PIDM-DCSK at various bit per symbols length for two symbols per frame where $M = 100$.

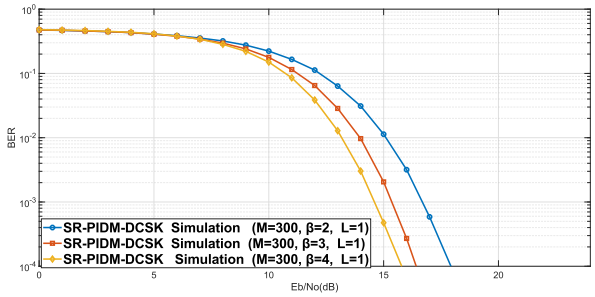

FIGURE 12. The BER results for SR-PIDM-DCSK at various bit per symbols length for one symbol per frame where $M = 300$.

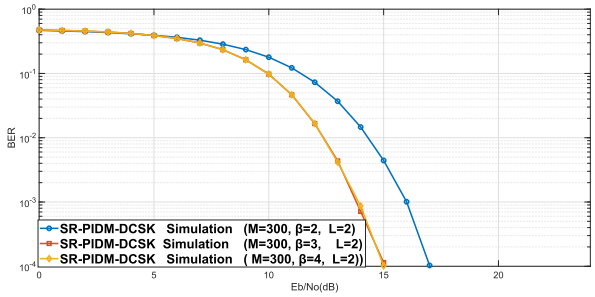

FIGURE 13. The BER results for SR-PIDM-DCSK at various bit per symbols length for two symbols per frame where $M = 300$.

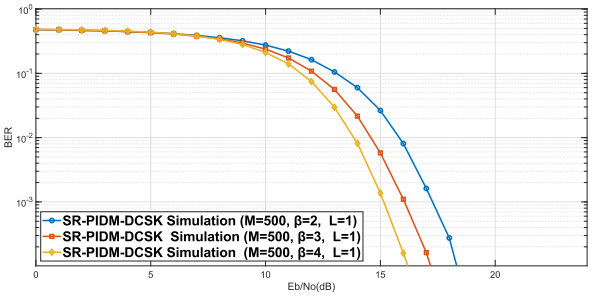

FIGURE 14. The BER results for SR-PIDM-DCSK at various bit per symbols length for one symbol per frame where $M = 500$.

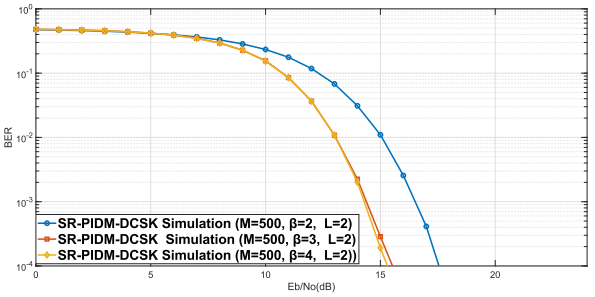

FIGURE 15. The BER results for SR-PIDM-DCSK at various bit per symbols length for two symbols per frame where $M = 500$.

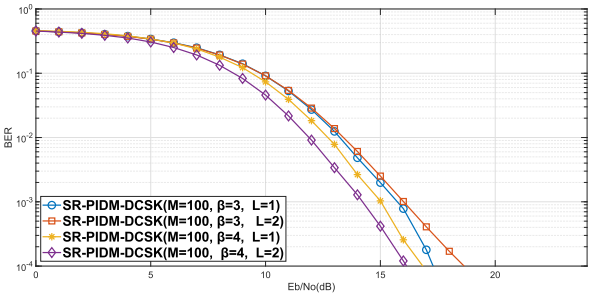

FIGURE 16. The BER results for SR-PIDM-DCSK at various bit per symbols length at single and double frames where $M = 100$.

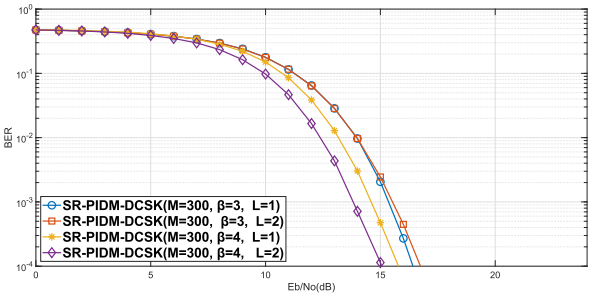

FIGURE 17. The BER results for SR-PIDM-DCSK at various bit per symbols length at single and double frames where $M = 300$.

due to noise to noise contribution that appears at the correlator output as indicated in Eq. (32)

The system is investigated with the various bits per symbols length, typically with 2, 3 and 4 bits per symbol as shown in Figs. 10, 11, 12, 13, 14 and 15 and at various spreading factors. Results clearly indicate that increasing the number of bits per symbol enhances the performance at various spreading factors. It is clearly note that the system performance is enhanced while the number of bits and frames are increased, predictably, as β increases the SR-PIDM-DCSK BER performance improved. This due to the fact that for higher β, more bits are mapped within a symbol for the same transmitted energy, hence the E_b/N_0 required to achieve a certain BER performance is reduced.

Increasing of frame length L also contributes positively to the system performance since in each frame, a symbol or

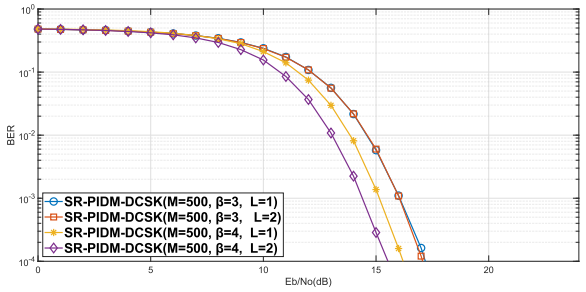

FIGURE 18. The BER results for SR-PIDM-DCSK at various bit per symbols length at single and double frames where $M = 500$.

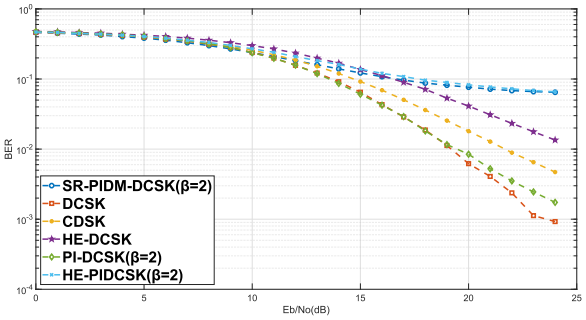

FIGURE 19. The BER results for SR-PIDM-DCSK verses DCSK, CDSK, HE-DCSK, PI-DCSK and HE-PIDCSK over multipath Rayleigh fading channels where $M = 100$ and $\zeta = 20$.

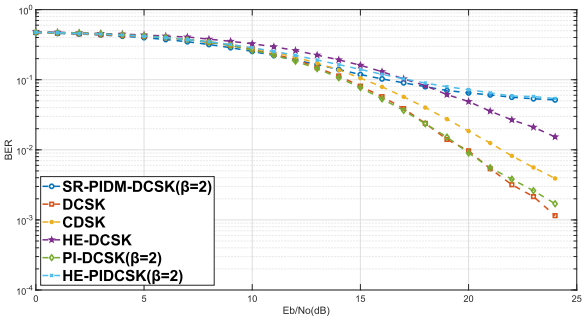

FIGURE 20. The BER results for SR-PIDM-DCSK verses DCSK, CDSK, HE-DCSK, PI-DCSK and HE-PIDCSK over multipath Rayleigh fading channels where $M = 200$ and $\zeta = 30$.

groups of symbols use the same reference chaotic segment, which reduces the energy requirement by almost half. System error performance is always enhanced by using larger frame size as shown in Figs. 16, 17 and 18 at fixed symbol length.

The BER performance is evaluated over two-ray Rayleigh fading channel. The transmitted signal can be written as $\rho_1 S + \rho_2 S_\zeta$ where ρ_1 and ρ_2 are selected fading channel coefficients with PDF Rayleigh distribution given by $f(\rho/\sigma) = \frac{\rho}{\sigma^2} e^{\frac{-\rho^2}{2\sigma^2}}$. Where σ is the root mean square value of the received signal. ζ is the delay factor equal to $0.2M$. It is important to mention that the channel coefficient is considered to be constant over one symbol duration.

The BER performance of the proposed system is compared with DCSK, CDSK, HE-DCSK, PI-DCSK and HE-PIDCSK at spreading factors 100, 150, 300 and 500 and with delay factor of $\zeta = 0.2M$.

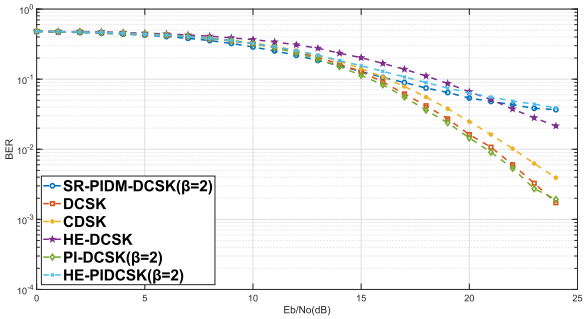

FIGURE 21. The BER results for SR-PIDM-DCSK verses DCSK, CDSK, HE-DCSK, PI-DCSK and HE-PIDCSK over multipath Rayleigh fading channels where $M = 300$ and $\zeta = 20$.

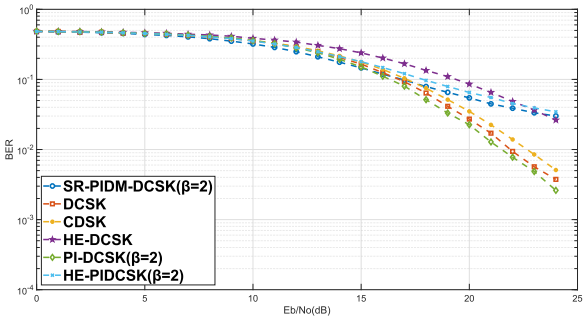

FIGURE 22. The BER results for SR-PIDM-DCSK verses DCSK, CDSK, HE-DCSK, PI-DCSK and HE-PIDCSK over multipath Rayleigh fading channels where $M = 500$ and $\zeta = 30$.

The system performance is compared with other permutation-based DCSK systems as shown in Figs. 19, 20, 21 and 22. The proposed system performance is very similar to the HE-PIDCK. The other systems outperform the proposed scheme due to the fact that the received signal from the multipath channels interfered with the previously transmitted symbols which directly affect the permutation characteristic of the signal. This can be addressed by adding a time guard between each transmitted frame.

VII. CONCLUSION

A new version of SR-PIDM-DCSK is designed and tested. The proposed system uses the chaotic segment and its reversed version to modulate two pairs of data sets simultaneously with the same reference for multiple symbol modulations. This is achieved by sending the reference signal first, followed by the delayed version of the reference and permutated information set of bits, while the same version is time reversed and permutated to modulate the second set of bits. Both segments are added together on the same symbol duration slot for transmission. At the receiver, the incoming reference signal is delayed for several symbol durations for demodulation. The system is modeled using based band representation and validated using simulation. BER performance of the system is simulated and evaluated with DCSK, CDSK, HE-PI-DCSK, HE-DCSK, and PI-DCSK schemes. Results illustrate that the system performance improves with the increasing of bits number per symbol and frame length. Moreover, the proposed system outperforms

the recent permutations-based chaos systems (HE-PI-DCSK) at large spreading factor by an average of 2 db. Based on the GA method, theoretical prediction for BER is developed and compared with the simulation results. Excellent matching between the derived form and simulation results was noticed.

REFERENCES

[1] G. Kolumban, M. P. Kennedy, and L. O. Chua, "The role of synchronization in digital communications using chaos. II. Chaotic modulation and chaotic synchronization," *IEEE Trans. Circuits Syst. I, Fundam. Theory Appl.*, vol. 45, no. 11, pp. 1129–1140, Nov. 1998.
[2] C. Tse and F. Lau, "Chaos-based digital communication systems," in *Operating Principles, Analysis Methods, and Performance Evaluation*. Berlin, Germany: Springe-Verlag, 2004, 2003.
[3] G. Kis, Z. Jako, M. Kennedy, and G. Kolumbán, "Chaotic communications without synchronization," Tech. Rep., 1998.
[4] G. Kolumban, Z. Jako, and M. P. Kennedy, "Enhanced versions of DCSK and FM-DCSK data transmission systems," in *Proc. IEEE Int. Symp. Circuits Syst.*, vol. 4, May 1999, pp. 475–478.
[5] H. Yang and G.-P. Jiang, "High-efficiency differential-chaos-shift-keying scheme for chaos-based noncoherent communication," *IEEE Trans. Circuits Syst. II, Exp. Briefs*, vol. 59, no. 5, pp. 312–316, May 2012.
[6] H. Yang and G.-P. Jiang, "Reference-modulated DCSK: A novel chaotic communication scheme," *IEEE Trans. Circuits Syst. II, Exp. Briefs*, vol. 60, no. 4, pp. 232–236, Apr. 2013.
[7] G. Kaddoum and F. Gagnon, "Design of a high-data-rate differential chaos-shift keying system," *IEEE Trans. Circuits Syst. II, Exp. Briefs*, vol. 59, no. 7, pp. 448–452, Jul. 2012.
[8] M. Xu and H. Leung, "A novel high data rate modulation scheme based on chaotic signal separation," *IEEE Trans. Commun.*, vol. 58, no. 10, pp. 2855–2860, Oct. 2010.
[9] P. Chen, L. Wang, and F. C. M. Lau, "One analog STBC-DCSK transmission scheme not requiring channel state information," *IEEE Trans. Circuits Syst. I, Reg. Papers*, vol. 60, no. 4, pp. 1027–1037, Apr. 2013.
[10] P. Chen, L. Shi, Y. Fang, G. Cai, L. Wang, and G. Chen, "A coded DCSK modulation system over Rayleigh fading channels," *IEEE Trans. Commun.*, vol. 66, no. 9, pp. 3930–3942, Apr. 2018.
[11] G. Kaddoum, F. Richardson, and F. Gagnon, "Design and analysis of a multi-carrier differential chaos shift keying communication system," *IEEE Trans. Commun.*, vol. 61, no. 8, pp. 3281–3291, Aug. 2013.
[12] T. Huang, L. Wang, W. Xu, and G. Chen, "A multi-carrier M-ary differential chaos shift keying system with low PAPR," *IEEE Access*, vol. 5, pp. 18793–18803, 2017.
[13] F. S. Hasan and A. A. Valenzuela, "Design and analysis of an OFDM-based orthogonal chaotic vector shift keying communication system," *IEEE Access*, vol. 6, pp. 46322–46333, 2018.
[14] B. Chen, L. Zhang, and Z. Wu, "General iterative receiver design for enhanced reliability in multi-carrier differential chaos shift keying systems," *IEEE Trans. Commun.*, vol. 67, no. 11, pp. 7824–7839, Nov. 2019.
[15] W. Hu, L. Wang, G. Cai, and G. Chen, "Non-coherent capacity of M-ary DCSK modulation system over multipath Rayleigh fading channels," *IEEE Access*, vol. 5, pp. 956–966, 2016.
[16] F. C. M. Lau, K. Y. Cheong, and C. K. Tse, "Permutation-based DCSK and multiple-access DCSK systems," *IEEE Trans. Circuits Syst. I, Fundam. Theory Appl.*, vol. 50, no. 6, pp. 733–742, Jun. 2003.
[17] K. Y. Cheong, F. C. M. Lau, and C. K. Tse, "Permutation-based M-ary chaotic-sequence spread-spectrum communication systems," *Circuits, Syst. Signal Process.*, vol. 22, no. 6, pp. 567–577, Dec. 2003.
[18] M. Herceg, G. Kaddoum, D. Vranjes, and E. Soujeri, "Permutation index DCSK modulation technique for secure multiuser high-data-rate communication systems," *IEEE Trans. Veh. Technol.*, vol. 67, no. 4, pp. 2997–3011, Apr. 2018.
[19] G. Cai, Y. Fang, J. Wen, S. Mumtaz, Y. Song, and V. Frascolla, "Multi-carrier M-ary DCSK system with code index modulation: An efficient solution for chaotic communications," *IEEE J. Sel. Topics Signal Process.*, vol. 13, no. 6, pp. 1375–1386, May 2019.
[20] M. Miao, L. Wang, G. Chen, and W. Xu, "Design and analysis of replica piecewise M-ary DCSK scheme for power line communications with asynchronous impulsive noise," *IEEE Trans. Circuits Syst. I, Reg. Papers*, vol. 67, no. 12, pp. 5443–5453, Dec. 2020.
[21] G. Cai and Y. Song, "Closed-form BER expressions of M-ary DCSK systems over multipath Rayleigh fading channels," *IEEE Commun. Lett.*, vol. 24, no. 6, pp. 1192–1196, Jun. 2020.
[22] M. Herceg, D. Vranjes, G. Kaddoum, and E. Soujeri, "Commutation code index DCSK modulation technique for high-data-rate communication systems," *IEEE Trans. Circuits Syst. II, Exp. Briefs*, vol. 65, no. 12, pp. 1954–1958, Dec. 2018.
[23] W. Xu, Y. Tan, F. C. M. Lau, and G. Kolumbán, "Design and optimization of differential chaos shift keying scheme with code index modulation," *IEEE Trans. Commun.*, vol. 66, no. 5, pp. 1970–1980, May 2018.
[24] H. Ma, G. Cai, Y. Fang, P. Chen, and G. Chen, "Design of a superposition coding PPM-DCSK system for downlink multi-user transmission," *IEEE Trans. Veh. Technol.*, vol. 69, no. 2, pp. 1666–1678, Feb. 2020.
[25] G. Cai, Y. Fang, P. Chen, G. Han, G. Cai, and Y. Song, "Design of an MISO-SWIPT-aided code-index modulated multi-carrier M-DCSK system for E-health IoT," *IEEE J. Sel. Areas Commun.*, vol. 39, no. 2, pp. 311–324, Feb. 2021.
[26] L. Stoica, A. Rabbachin, and I. Oppermann, "A low-complexity noncoherent IR-UWB transceiver architecture with TOA estimation," *IEEE Trans. Microw. Theory Techn.*, vol. 54, no. 4, pp. 1637–1646, Jun. 2006.
[27] N. A. Bassam, O. Al-Jerew, and A. Al-Qaraghuli, "High efficiency scheme for permutation index differential coherent chaos-based communication system," in *Proc. IEEE 63rd Int. Midwest Symp. Circuits Syst. (MWSCAS)*, Aug. 2020, pp. 782–785.

NIZAR AL BASSAM received the M.Sc. degree from AlMustnsryia University, in 2000, and the Ph.D. degree in modern communication systems from Al Nahrain University, in 2004. He is currently the Head of the Research and Consultancy Centre, Middle East College. He worked in many funded research projects related to chaos-based communications and the IoT. His research interests include spread spectrum communications, chaos-based communications, and the IoT. He has authored or coauthored many scientific publications, including journal articles, conference proceedings papers, and book chapters in these fields. He is an Editorial Member of the Board of the *Journal of Big Data and Smart City* and the technical chair and technical committee member of several international conferences.

ODAY AL-JEREW received the B.Sc. degree in computer and control engineering and the M.S. degree in computer engineering from the University of Technology, Baghdad, Iraq, in 1997 and 2000, respectively, and the Ph.D. degree in information technology from the College of Engineering and Computer Science, Australian National University (ANU), Canberra, Australia, in 2012. From 2012 to 2013, he was a Research Fellow at ANU. He was involved in many projects and gained extensive industrial experience during his work at industrial companies. He worked as a software and systems developer at robotics company to develop embedded applications for mobile robots. Also, he designed and developed microcomputer-based systems. He is currently the Head of the information technology discipline at Asia Pacific International College (APIC), Australia. His research interests include the development of routing algorithms for mobile *ad hoc* and wireless sensor networks to improve the network lifetime, and the design of chaos-based systems.